

On sublayer streaks

By M. T. LANDAHL

Department of Aeronautics and Astronautics, Massachusetts Institute of Technology,
Cambridge, MA 02139, USA

(Received 30 June 1989)

Turbulent sublayer streaks are studied with the aid of a simplified theoretical model. In this the nonlinear activity is assumed to be intermittent and to act locally in space during a very short initial time so as to set up the initial conditions for the subsequent linear and inviscid evolution of the resulting three-dimensional flow disturbance. The mean shear flow is taken as a parallel one and a correction for the long-term effects of viscosity is applied. A model for the initial nonlinear phase is chosen to represent the local Reynolds stresses that would be produced by a patch of local inflectional instability. The streamwise dimension of the resulting eddy is found to grow linearly with time in accordance with the algebraic instability mechanism (Landahl 1980). The associated Reynolds shear stress is expressible in a simple manner in terms of the liftup of the fluid elements and is suggestive of an algebraic-type Reynolds stress model similar to, but not identical to, that of Prandtl's (1925) mixing-length theory.

1. Introduction

One of the most outstanding characteristics of the near-wall turbulence structure in a boundary layer or channel flow is the presence of streamwise streaks of low- and high-speed regions (often referred to in the literature as 'streamwise vortices'). Their significance was first clearly brought out by the flow visualization experiments of Kline *et al.* (1967). The near-wall turbulence structure has since then become the subject of extensive studies by many researchers. In recent years these have been greatly aided by the availability of numerically simulated turbulent flows such as those obtained by Moin & Kim (1982), see e.g. the investigation by Alfredsson, Johansson & Kim (1988). Streamwise streaks are found also in other flows such as in the laminar region behind a turbulent transition spot as well as in turbulent mixing layers. Thus, streak formation appears to be a phenomenon common to many shear flows, but its cause is little understood.

Most of the efforts to date to give a theoretical explanation for the streaks have been concerned with their average spanwise spacing. These efforts have met with some limited success. Bark's (1975) calculation of the wavenumber–frequency spectrum of the streamwise velocity fluctuations in a boundary layer with the use of the wave-guide model (Landahl 1967) gave a peak of the streamwise fluctuation spectrum at a spanwise wavenumber corresponding to a streak spacing of about 150 in viscous wall units, which is to be compared to the experimental value of about 100. Jang, Benney & Gran (1986) proposed that the streak formation is a result of a resonance between the vertical vorticity mode (the 'Squire mode') and the Orr–Sommerfeld mode. They found that such a resonance could occur at a spanwise wavenumber corresponding to a streak spacing of 90 in viscous units, and they were

also able to compute a resulting streamwise vortex pattern in qualitative agreement with experiments. In their calculations based on rapid distortion theory, Lee & Hunt (1988) found a spanwise spacing about equal to the initial turbulence lengthscale with the spacing increasing with the distance from the wall.

In their study of the wall structure, Hatzivramidis & Hanratty (1979) applied a '2½-dimensional' model in which the cross-flow velocity (v, w) field was approximated as a two-dimensional one in the cross-flow (y, z) plane. The flow near the wall was considered driven by the fluctuating pressures originating from the action of the flow outside wall region which was represented as a periodic one with a spanwise lengthscale of 100 viscous units. From this model, they found good agreement with measured statistical properties, particularly for $y^+ < 15$. The model has been further refined in the later papers from Hanratty's group.

The problem of the generation and maintenance of the turbulent fluctuations in a boundary layer was addressed by Landahl (1975). By considering the interaction between disturbances of widely different scales, he showed that, in a flow of small viscosity, a large-scale disturbance, which could be initiated by a patch of small-scale instability arising in a region of inflectional velocity distribution, would form an almost permanent 'scar' of velocity defect or excess. In a later paper analysing the evolution of linear three-dimensional disturbances in a parallel inviscid shear flow (Landahl 1980) he demonstrated that, for a certain wide class of initial disturbances, the streamwise dimension of the disturbed region will grow at a constant rate and thereby give a total disturbance energy which is proportional to time. This algebraic-type instability can arise in all inviscid shear flows, whether stable or not in the Rayleigh sense; however, for flows with inflection the algebraic growth will of course eventually be swamped by the exponential one.

In the present paper the evolution of streamwise streaks is studied with the possible role of algebraic instability kept in mind. A simplified model is set up in which nonlinearity is assumed to act only during short intermittent 'bursting' intervals of local instability, thereby setting up the initial conditions for the subsequent linear evolution of the disturbances created. The long-term effects of viscosity are incorporated in an approximate fashion. It is found from this model that disturbances with spanwise asymmetry will grow into streaks, in consistency with algebraic instability, and that their structures show remarkable similarity with those observed in experiments and in numerical simulations.

2. Basic formulation of the model

The flow considered is modelled as a parallel mean shear flow $\bar{U}\delta_{i1}$, onto which is superimposed an unsteady three-dimensional disturbance with velocity $u_i(x_j, t)$ and pressure $p(x_i, t)$. The coordinate system used is the usual one in boundary layer theory with $x_1 = x$ in the mean streamwise direction, $x_2 = y$ normal to the wall (located at $y = 0$), and $x_3 = z$ in the spanwise direction (figure 1). From the Navier-Stokes equations the following equations for the disturbed flow field are obtained:

$$U_i(x_j, t) = \bar{U}(y)\delta_{i1} + u_i(x_j, t), \quad (1)$$

$$\frac{D u_i}{Dt} + \bar{U}'(y) u_2 \delta_{i1} = -\frac{1}{\rho} \left[\frac{\partial p}{\partial x_i} + \frac{\partial}{\partial x_j} \left(\mu \frac{\partial u_i}{\partial x_j} + \tau_{ij} \right) \right], \quad (2)$$

$$\frac{\partial u_i}{\partial x_i} = 0, \quad (3)$$

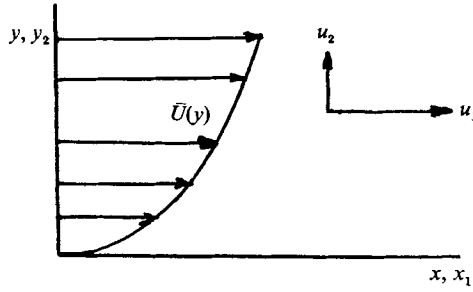


FIGURE 1. Coordinate system.

where
$$\frac{\bar{D}}{Dt} = \frac{\partial}{\partial t} + \bar{U} \frac{\partial}{\partial x}, \tag{4}$$

$$\tau_{ij} = -\rho(u_i u_j - \bar{u}_i \bar{u}_j). \tag{5}$$

Elimination of the pressure gives (Landahl 1967)

$$\frac{\bar{D}\nabla^2 v}{Dt} - v_x \bar{U}'' - \nu \nabla^4 v = q, \tag{6}$$

where
$$q = \nabla^2 T_2 - \frac{\partial^2 T_i}{\partial x_i \partial x_2} \approx \frac{\partial^2}{\partial y^2} \left[\frac{\partial}{\partial x} (uv) + \frac{\partial}{\partial z} (vw) \right] + \dots, \tag{7}$$

$$T_i = \frac{1}{\rho} \frac{\partial \tau_{ij}}{\partial x_j}, \tag{8}$$

which may be viewed as a non-homogeneous Orr–Sommerfeld equation in which the nonlinear terms provide, through q , the random forcing. In view of the expected boundary-layer character of the fluctuations one may anticipate that the nonlinear terms singled out, which contain the highest y -derivatives, would be the dominating ones near the wall.

3. Some idealized models

From the above basic formulation a number of different idealized models may be constructed, each with its own range of applicability.

For very weak disturbances one could consider the use of *linear theory*

$$\frac{\bar{D}\nabla^2 v}{Dt} - \bar{U}'' \frac{\partial v}{\partial x} - \nu \nabla^4 v = 0. \tag{9}$$

This theory has been found to describe adequately the evolution of forced oscillatory disturbances in a turbulent free shear layer (Gaster, Kit & Wygnanski 1985). This flow, being inflectional in the mean, is inviscidly unstable, and the linear interaction between the disturbances and the mean shear flow theory thus appears to capture an essential part of the turbulence mechanism. For a shear flow that is linearly stable to small disturbances, however, disturbances cannot arise by themselves through linear instability, and one would have to consider some alternative means of initiation of the disturbance, by some outside means or through the local effect of nonlinearities.

Application of Fourier transform to (6) yields an equation with a linear

Orr–Sommerfeld operator on the left-hand side. Regarding the right-hand ‘source’ term, q , as given, one may treat the flow as a linear system forced in a random manner by the nonlinear interaction between the velocity fluctuation components. On the assumption that the spectrum of q is reasonably flat, one finds from this wavenumber–frequency spectra dominated by the lightly damped Orr–Sommerfeld waves near resonance (the *wave-guide model*, Landahl 1967; Bark 1975). The spectral representation is not very useful for the treatment of the space–time evolution of a coherent structure, however, the Orr–Sommerfeld modes not being particularly well suited for the representation of an initial disturbance of an arbitrary form (for a boundary layer they do not form a complete set, for example).

For short times after the creation of a flow structure, the effects of viscosity may be neglected. Hence one may work with the *inviscid model*

$$\frac{\bar{D}\nabla^2 v}{Dt} - \bar{U}'' \frac{\partial v}{\partial x} = q, \quad (10)$$

which for fluids of small viscosity may be applicable for fairly long evolutionary times. However, even a small viscosity will eventually become important for very long times and we will consider its long-time effects later.

An instructive model for the study of the qualitative effects of nonlinearities is the inviscid *flat-eddy* model of Russel & Landahl (1984), in which horizontal pressure gradients are neglected,

$$\frac{D(u + \bar{U})}{Dt} = 0, \quad \frac{D}{Dt} = \frac{D}{Dt} + u_j \frac{\partial}{\partial x_j}, \quad (11)$$

$$\frac{Dw}{Dt} = 0, \quad (12)$$

which was found to give a singularity at a finite time after the initiation of the structure, manifesting itself as a local outflow of infinite strength with a flow pattern resembling that seen in ejections from the wall region (see Landahl & Henningson 1985).

An approximation that has been applied with considerable success for the study of the evolution of spectra of turbulent flows going through region of strong shear and rapid acceleration/decelerations is the *rapid distortion theory* (see e.g. Townsend 1976), which for the shear-flow case may be obtained by neglecting all nonlinear (and usually also viscous) terms in (6) and setting the mean shear constant, so that $\bar{U}'' = 0$, giving

$$\frac{\bar{D}\phi}{Dt} - \nu \nabla^2 \phi = 0, \quad (13)$$

where

$$\phi = \nabla^2 v, \quad (14)$$

which may be integrated over time so as to produce the Poisson equation (14) for v directly expressible in terms of the initial conditions. This may be solved by standard methods and spectra are hence readily constructed. However, because of the neglect of nonlinear mechanisms, rapid distortion theory only holds for the short- and medium-length time of spectral evolution. It does not yield a steady-state solution.

A formulation related to that of rapid distortion theory is the one obtained by assuming *nonlinear intermittency*, giving

$$\frac{\bar{D}\nabla^2 v}{Dt} - \bar{U}'' \frac{\partial v}{\partial x} - \nu \nabla^4 v = q, \quad (15)$$

with

$$q = Q_n(x, y, z) \delta(t - t_n), \tag{16}$$

and where $t = t_n$ are the ‘bursting’ instants. As will be seen below, one may formulate this problem as a linear initial-value problem with the initial conditions set by the nonlinear activity at $t = t_n$. Statistical data from the near-wall region (Moin & Kim 1982) show that the v -component is highly intermittent (but not the u -component) as indicated by the extremely large flatness exhibited by its distribution function.

In view of the observation that the near-wall turbulent flow contains structures of widely varying scales, which may interact in an important manner despite their large scale separation, it may be interesting to consider a model employing *scale subdivision* with the large scales accounting for the coherent structures and the small scales involving the incoherent background. Such a scale subdivision yields the following pair of equations (Landahl 1975):

$$\bar{u}_i = \underbrace{\tilde{u}_i}_{\text{‘large-scale coherent’ field}} + \underbrace{u'_i}_{\text{‘random non-coherent’}}, \quad \tilde{u}'_i = 0, \tag{17}$$

$$\frac{\tilde{D}\nabla^2\tilde{v}}{Dt} - \tilde{U}'' \frac{\partial\tilde{v}}{\partial x} - \nu\nabla^4\tilde{v} = \tilde{q}' + \tilde{q}, \tag{18}$$

where

$$\tilde{U} = U + \tilde{u}, \tag{19}$$

$$\frac{\tilde{D}}{Dt} = \frac{D}{Dt} + \tilde{u}_j \frac{\partial}{\partial x_j}, \tag{20}$$

$$\tilde{q}' \approx \frac{\partial^2}{\partial y^2} \left[\frac{\partial}{\partial x} (u'v') + \frac{\partial}{\partial z} (v', w') \right], \tag{21}$$

$$\frac{\tilde{D}\nabla^2 v'}{Dt} - \tilde{U}_{yy} v'_x - \tilde{u}_{yy} v'_z - \nu\nabla^4 v' = q'. \tag{22}$$

The small scales could be initiated by local instability, for example, in regions where the large-scale flow develops inflection. Then, for the small-amplitude case the right-hand side of (22) may be neglected leading to an Orr–Sommerfeld-type equation but with slowly varying coefficients in time and horizontal space. This could be handled with the aid of kinematic wave theory.

4. Model for the streaky structure

In view of the observations that the vertical component of the fluctuating velocity field is highly intermittent we will adopt the intermittency formulation given above and apply it to an inviscid disturbance,

$$\frac{\tilde{D}\phi}{Dt} - \tilde{U}'' \frac{\partial\phi}{\partial x} = Q_n(x, y, z) \delta(t - t_n). \tag{23}$$

Integration over time from $t = t_n - 0$ to $t = t_n + 0$ gives

$$\phi \equiv \nabla^2 v = Q_n(\xi_n, y, z) + \tilde{U}'' \frac{\partial l}{\partial x}, \tag{24}$$

in which

$$\xi_n = x - \tilde{U}(y) (t - t_n) \tag{25}$$

and where
$$l = \int_{t_n}^t v(x_1, y, z, t_1) dt_1, \tag{26}$$

$$x_1 = x - \bar{U}(y)(t - t_1). \tag{27}$$

Here l is the fluid-element liftup in linear approximation, cf. Prandtl (1925). For $t > t_n$ one may formulate the problem as an initial-value one with

$$\frac{\bar{D}\nabla^2 v}{Dt} - \bar{U}'' \frac{\partial v}{\partial x} = 0 \tag{28}$$

and, on the assumption that $l = 0$ for $t = t_n$,

$$\phi = \phi_n = \nabla^2 v_n = Q_n(x, y, z) \quad \text{for } t = t_n + 0. \tag{29}$$

Inversion of the Laplacian gives

$$v = -\frac{1}{4\pi} \int_{-\infty}^{\infty} dx_1 \int_{-\infty}^{\infty} dz_1 \int_0^{\infty} \phi(x_1, y_1, z_1, t) \left(\frac{1}{R_1} - \frac{1}{\bar{R}_1} \right) dy_1, \tag{30}$$

where

$$R_1 = [(x - x_1)^2 + (y - y_1)^2 + (z - z_1)^2]^{\frac{1}{2}}, \tag{31}$$

$$\bar{R}_1 = [(x - x_1)^2 + (y + y_1)^2 + (z - z_1)^2]^{\frac{1}{2}} \tag{32}$$

and where $\phi(x, y, z; t)$ is given by (24), (25). The fluid-element liftup, l , may be obtained from (26) by direct integration. After a reversal of the orders of integration one finds the following result:

$$l = -\frac{1}{4\pi} \int_{-\infty}^{\infty} dx_1 \int_{-\infty}^{\infty} dz_1 \int_0^{\infty} \frac{P - P^*}{\bar{U} - \bar{U}_1} \left(\frac{1}{R_1} - \frac{1}{\bar{R}_1} \right) dy_1, \tag{33}$$

where
$$P(x_1, y_1, z_1; t) = \int_{-\infty}^{\xi_1} Q_n(x_2, y_1, z_1) dx_2 + \bar{U}''(y_1) l(x_1, y_1, z_1; t), \tag{34}$$

with

$$\xi_1 = x_1 - \bar{U}(y_1)(t - t_n)$$

and where

$$P^*(x_1, y_1, y, z_1; t) = \int_{-\infty}^{\xi^*} Q_n(x_2, y_1, z_1) dx_2 + \bar{U}''(y_1) l^*(x_1, y, y_1, z_1; t), \tag{35}$$

$$l^* = \int_{t_n}^t v(\xi^{**}, y_1, z_1, t_1) dt_1 \tag{36}$$

with
$$\xi^* = x_1 - \bar{U}(y)(t - t_n), \quad \xi_1^{**} = x_1 - \bar{U}(y_1)(t - t_n).$$

For the streamwise fluctuation component one has

$$\frac{\bar{D}u}{Dt} = -v\bar{U}'(y) - \frac{1}{\rho} \frac{\partial p}{\partial x} \text{ (+ nonlinear terms)}. \tag{37}$$

The pressure may be obtained from the divergence of the horizontal perturbation momentum equations which gives

$$\nabla_{\perp}^2 \left(\frac{p}{\rho} \right) = \frac{\bar{D}v_y}{Dt} - v_x \bar{U}' \text{ (+ nonlinear terms)} \tag{38}$$

(subscripts x and y denoting partial derivatives), where

$$\nabla_{\perp}^2 \equiv \frac{\partial^2}{\partial x^2} + \frac{\partial^2}{\partial z^2}. \tag{39}$$

Let the inverse of the two-dimensional Laplace operator be defined by $L^{-1}(f)$, where

$$L^{-1}(f(x, z)) = \frac{1}{4\pi} \int_{-\infty}^{\infty} dx_1 \int_{-\infty}^{\infty} f(x_1, z_1) \log [(x-x_1)^2 + (z-z_1)^2] dz_1. \quad (40)$$

With $V = L^{-1}(v)$, $L = L^{-1}(l)$ (41)

one then finds from (37) that

$$u = u_n(\xi_n, y, z) - l\bar{U}'(y) - \frac{\partial}{\partial x} [V_y - V_{yn}(\xi_n, y, z) - L_x \bar{U}'] \quad (+ \text{nonlinear terms}), \quad (42)$$

subscript n denoting values at $t = t_n$ as before. For structures that are highly elongated in the streamwise direction $\nabla_n^2 \approx \partial^2 / \partial z^2$, and one has

$$V \approx \int_{-\infty}^z (z-z_1) v(x; y, z_1) dz_1. \quad (43)$$

For such structures the pressure gradient term will give a contribution to the streamwise perturbation velocity which is of the order $(l_3/l_1)^2$ times that coming from the first term and hence negligible, giving

$$u \approx u_n(\xi_n, y, z) - \bar{U}(y) l \quad (44)$$

(cf. Prandtl 1925). The first term represents a purely convected part of the disturbance with $v = 0$, which will be considered separately below. In the calculations of the long-time evolution of the structure to be presented below it will be assumed that $u_n = 0$.

On the other hand, for structures that vary little with z , i.e. are nearly two-dimensional,

$$V \approx \int_{-\infty}^x (x-x_1) v(x_1; z) dx_1, \quad (45)$$

then $u \approx - \int_{-\infty}^x v_y(x_1; z) dx_1$ (46)

in consistency with continuity.

For the study of the evolution of a highly three-dimensional structure of interest here it is convenient to set

$$v = v_{\text{trans}} + v_{\text{inter}}, \quad (47)$$

where

$$v_{\text{trans}} = -\frac{1}{4\pi} \int_{-\infty}^{\infty} dx_1 \int_{-\infty}^{\infty} dz_1 \int_0^{\infty} Q_n(\xi_n, y_1, z_1) \left(\frac{1}{R_1} - \frac{1}{\bar{R}_1} \right) dy_1, \quad (48)$$

$$v_{\text{inter}} = -\frac{1}{4\pi} \int_{-\infty}^{\infty} dx_1 \int_{-\infty}^{\infty} dz_1 \int_0^{\infty} \bar{U}''(y_1) l_x(x_1, y_1, z_1; t) \left(\frac{1}{R_1} - \frac{1}{\bar{R}_1} \right) dy_1. \quad (49)$$

For small times the disturbance is dominated by its transient part which may be found directly from the initial distribution. The interactive part is zero for $\bar{U}' = \text{const.}$, and the result then becomes identical to that of rapid distortion theory. For a non-zero \bar{U}'' , the interactive part of the solution must be determined by a step-by-step integration in time. This was done in the numerical examples presented below with the use of a specially developed explicit method having second-order accuracy. For small and moderate times the transient part alone (which gives results in agreement with rapid distortion theory) is found to represent the solution in a qualitatively satisfactory way. As will be demonstrated below, for very long times the disturbance will evolve into a pair of streamwise streaks.

5. Long-time behaviour – the role of algebraic instability

The long-time structure of the disturbance may be directly inferred from the solution (33)–(36). Consider an initial local disturbance of streamwise length $2L$ confined between $x > -L$ and $x < L$. Also, set

$$\int_{-\infty}^{\infty} Q_n(x_1, y, z) dx_1 = P_{n\infty}(y, z), \quad (50)$$

where $P_{n\infty}$ is assumed to be non-zero. Then, following (33), for large t there will be a streamwise region of length $\Delta x_1 = |\bar{U} - \bar{U}_1|t - 2L$ for which the contribution to the integrand from the initial condition will become independent of x_1 . Also, the contribution from the term in (33) proportional to \bar{U}'' is likely to be small, since for a stable mean profile v vanishes as t approaches infinity and, furthermore, the streamwise average of the term is zero. Hence, for large times, the flow will tend to become two-dimensional in the cross-flow (y, z) plane over a streamwise length growing linearly with time.

This phenomenon is related to the concept of algebraic instability explored by Landahl (1980). He showed through streamwise averaging of the perturbation equations that for an inviscid shear flow without inflection, having $u = u_0, v = v_0$, for $t = 0^+$,

$$\int_{-\infty}^{\infty} v(x, y, z, t) dx = \int_{-\infty}^{\infty} v_0(x, y, z) dx, \quad (51)$$

$$\int_{-\infty}^{\infty} u(x, y, z, t) dx = -t\bar{U}'(y) \int_{-\infty}^{\infty} v_0(x, y, z) dx + \int_{-\infty}^{\infty} u_0(x, y, z) dx. \quad (52)$$

It follows from this that, for an inviscid shear flow that is stable in the Rayleigh sense, the total streamwise momentum, and the perturbation energy, will grow linearly in time for all times after the initiation of the disturbance. As it is clear from the above analysis, the amplitude of the disturbance does not grow for all times, instead the streamwise length of the disturbance continues to grow linearly in time. Of course, in a real viscous fluid this growth will eventually cease. Nevertheless, for a fluid of small viscosity the flow will admit a substantial algebraic growth before the slow viscous decay takes over, in particular if the mean shear is large (the long-time effects of viscosity will be addressed later). Therefore, three-dimensional disturbances initially localized in the spanwise direction will evolve into highly elongated ones, i.e. will produce streaky structures having a large ratio of streamwise to spanwise dimensions. For the calculation of the long-time behaviour of such eddies it is appropriate to employ the 'slender-body' approximation, familiar in aerodynamics (see e.g. Ashley & Landahl 1965). It reduces the triple integral in (30) to a two-dimensional one in which the streamwise variable only enters parametrically, i.e.

$$v \approx \frac{1}{2\pi} \int_0^{\infty} dy_1 \int_{\infty}^{\infty} \phi(\xi_n, y_1, z_1; t) \ln(r_1/\bar{r}_1) dz_1, \quad (53)$$

$$r_1 = [(y - y_1)^2 + (z - z_1)^2]^{\frac{1}{2}}, \quad (54)$$

$$\bar{r}_1 = [(y + y_1)^2 + (z - z_1)^2]^{\frac{1}{2}}. \quad (55)$$

Very close to the wall the solution may be simplified even further so as to be expressible through the following line integrals;

$$v = \int_0^y \phi(\xi_n, y_1, z) (y - y_1) dy_1 - y \int_0^{\infty} \phi(\xi_n, y_1, z) dy_1. \quad (56)$$

The numerical results presented below are all based on the near-wall approximation (56).

6. Reynolds stresses

It is of interest to determine the contribution from the streaks to the mean Reynolds shear stress. This will be done on the basis of linear inviscid theory. The gradient of the turbulent shear stress is obtained from the average of

$$-\frac{\partial}{\partial y}(uv) = -uv_y - u_y v. \tag{57}$$

We want to determine the contribution from each streak by integration over time and horizontal space. It is convenient to express this in terms of the liftup variable l . By introducing (42) and neglecting the terms involving streamwise derivatives one finds (taking $u_n = 0$) after integration with respect to time

$$-\int_0^t \frac{\partial}{\partial y}(uv) dt = \frac{1}{2} \frac{\partial}{\partial y}[l^2 \bar{U}'(y)] \tag{58}$$

or
$$-\int_{-\infty}^{\infty} dx \int_{-\infty}^{\infty} dz \int_0^t (uv) dt = \frac{1}{2} \bar{U}'(y) \int_{-\infty}^{\infty} dx \int_{-\infty}^{\infty} l^2 dz, \tag{59}$$

which differs from Prandtl's (1925) famous formula

$$-\langle uv \rangle = l_m^2 (\bar{U}'(y))^2, \tag{60}$$

l_m being the root-mean square of l . Prandtl obtained this result under the assumption that $v \approx -u$. For a two-dimensional flow one finds in a similar manner that

$$-\int_0^t \frac{\partial}{\partial y}(uv) dt = \frac{1}{2} l^2 \bar{U}''(y), \tag{61}$$

which is equivalent to Taylor's (1915) result obtained from the vorticity transport equations. On taking the streamwise average and noting from (50) that for large t the integrand in (33) is constant in x and equal to $P_\infty = \int_{-\infty}^{\infty} Q_n dx$ over a distance equal to $|\bar{U} - \bar{U}_1|t$ one finds that

$$\begin{aligned} &-\int_{-\infty}^{\infty} dx \int_{-\infty}^{\infty} dz \int_0^t (uv) dt \\ &= \frac{1}{2} t \bar{U}'(y) \int_0^{\infty} H(y, y_1) P_{n\infty}(y_1; z) dy_1 \int_0^{\infty} H(y, y_2) P_{n\infty}(y_2; z) dy_2, \end{aligned} \tag{62}$$

where, in the near-wall approximation,

$$H(y, y_1) = 0.5(|y - y_1| - y - y_1). \tag{63}$$

In this inviscid flow model the shear stress contributed by a single streak thus continues to grow linearly in time for all times, in consistency with the prediction of algebraic instability theory. That the linear inviscid theory gives a Reynolds stress that grows linearly with time was found also by Moffatt (1965) in an analysis based on rapid distortion theory. In a real flow the viscosity will of course eventually make the streak decay, but for a fluid of low viscosity this is a very slow process. More likely, the streak will suffer breakup due to local inflectional instabilities in a finite

lifetime. The long-term effects of viscosity and secondary instability will be discussed further below.

For the total average Reynolds stress contributed by the near-wall streaks one thus has

$$-\langle uv \rangle = \frac{t_b}{2T_b} \bar{U}'(y) \int_0^\infty dy_1 \int_0^\infty H(y, y_1) H(y, y_2) R(y_1, y_2) dy_2, \quad (64)$$

where t_b and T_b are, respectively, the average lifetime of the streak and the time between bursts, and where

$$R(y_1, y_2) = \langle P_{n\infty}(y_1, z) P_{n\infty}(y_2, z) \rangle, \quad (65)$$

$\langle \rangle$ denoting ensemble average. It follows from (63) and (64) that the Reynolds stress varies like y^2 for small y . This supports the model proposed recently by Haritonidis (1989). For large y , $R(y_1, y_2)$ will become a function of $y_1 - y_2$ only (cf. the random-walk problem), and the average Reynolds stress will then become proportional to $y\bar{U}'$. In the constant-stress region this will lead to a logarithmic mean velocity profile.

7. Conditional sampling

For the study of coherent structures it is necessary to apply conditional sampling techniques in order to bring out the characteristic features of the structures of interest. Since the model evolution equations developed are linear, the averaging over the sample leads to a simple linear superposition of the individual events selected by the sampling criterion applied, giving

$$\langle v \rangle = -\frac{1}{4\pi} \int_{-\infty}^\infty dx_1 \int_{-\infty}^\infty dz_1 \int_0^\infty \langle \phi(\xi_1, y_1, z_1) \rangle \left(\frac{1}{R_1} - \frac{1}{\bar{R}_1} \right) dy_1, \quad (66)$$

$$\langle \phi(\xi, y, z) \rangle = \frac{1}{N} \sum_{i=1}^N \phi_n(\xi_n, y, z), \quad N \rightarrow \infty, \quad (67)$$

$$\xi = x - \bar{U}(y)(t - t_{\text{event}}); \quad \xi_1 = x - \bar{U}(y_1)(t - t_{\text{event}}), \quad (68)$$

from which the sampled fluid-element liftup $\langle l \rangle$ and hence the sampled streamwise velocity

$$\langle u \rangle = \langle u_n(\xi_n, y, z) \rangle - \bar{U}'(y) \langle l \rangle \quad (69)$$

may be obtained.

A sampling method that has been used with some success in the literature is the variable interval time averaging (VITA) sampling criterion (Blackwelder & Kaplan 1976), which sorts out events for which the local variance, evaluated for a selected time interval, T , exceeds a preset threshold factor, k , times the mean-square fluctuation level of the streamwise velocity component, i.e.

$$\text{var}(u, T) \equiv \frac{1}{T} \left[\int_{t_e - \frac{1}{2}T}^{t_e + \frac{1}{2}T} u^2 dt \right] - \left[\frac{1}{T} \int_{t_e - \frac{1}{2}T}^{t_e + \frac{1}{2}T} u dt \right]^2 > k u_{\text{rms}}^2. \quad (70)$$

As pointed out by Johansson & Alfredsson (1982), the integration time acts primarily as a filter so that small T tends to sort out events that are short-lived, whereas large T singles out long-lived events. Since the measurements are carried out in a fixed laboratory frame of reference, a short-lived event has a corresponding short streamwise scale, and vice versa for the long-lived ones.

The application of such a criterion supplies only the instants of the events around

which the sampling is done. It has been found that the sampled signal normalized with the root-mean-square fluctuation amplitude and with the square root of the threshold k is approximately independent of the threshold level (Blackwelder & Kaplan 1976). Landahl (1984) has shown that this is consistent with a linear model.

8. Convected eddy

For an inviscid shear flow without inflection a linear disturbance will decay at a rate faster than t^{-1} . Hence, for long times, $p \rightarrow 0$ and the equation for u becomes simply

$$\frac{\bar{D}u}{Dt} = 0, \tag{71}$$

with the solution

$$u = u_\infty(\xi, y, z), \quad \xi = x - \bar{U}(y)t, \tag{72}$$

where u_∞ is the final distribution of the u -perturbation velocity after the initial formation period with non-zero v has subsided. The result (72) is nothing but a statement of Taylor's 'frozen field' hypothesis. The shear due to such a disturbance,

$$\frac{\partial u}{\partial y} = -t\bar{U}'(y)u_{\infty\xi} + u_{\infty y}, \tag{73}$$

thus intensifies linearly with time and leads to the formation of internal shear layers in regions where $u_{\infty\xi} < 0$, which may with time become susceptible to local inflectional instability, as noticed by Gill (1965). An alternative explanation of the formation of the shear layers is through stretching of the spanwise mean vorticity by the spanwise perturbation velocity gradient w_z (note that, from continuity, $w_z = -u_{\infty\xi}$ with $v = 0$). However, because of the continuous increase in shear, the viscous shearing stresses will eventually become important, and one needs to consider the diffusion equation

$$\frac{\bar{D}u}{Dt} - \nu \nabla^2 u = 0. \tag{74}$$

The effects of a small viscosity may be determined in a simple approximate manner by setting

$$u = F(\xi, y, z, t), \tag{75}$$

which for large times gives

$$\nabla^2 u = t^2(\bar{U}')^2 F_{\xi\xi} + O(t) + O(1). \tag{76}$$

After application of the transformation

$$T = \frac{1}{3}\nu t^2(\bar{U}')^2 t^3 \tag{77}$$

and neglect of the unimportant terms at large times, one obtains

$$F_T - F_{\xi\xi} = 0, \quad F(\xi, y, z, 0) = u_\infty. \tag{78}$$

This may be solved with the aid of the standard methods for the heat equation. For an initial disturbance in the form of a Gaussian 'hat',

$$u_\infty \sim \exp\left[-\left(\frac{\xi}{l_1}\right)^2\right], \tag{79}$$

of streamwise scale l_1 one obtains the simple result (Landahl 1984) that

$$u \sim (l_1/L) \exp[-(\xi/L)^2], \quad (80)$$

where

$$L = [l_1^2 + \frac{4}{3}\nu(\bar{U}')^2 t^3]^{\frac{1}{2}}. \quad (81)$$

This result shows that the viscosity simply tends to make the disturbance grow in the streamwise direction and to decay at the same rate so as to keep the total streamwise momentum defect constant. Following this, in the calculations presented here the effects of viscosity are approximated simply by stretching continuously the streamwise dimension of the structure according to (81) and simultaneously reducing the amplitude by the factor (l_1/L) .

It follows from (80), (81) that the maximum shear occurs after a finite time given by

$$t = (\frac{3}{2}l_1^2 \nu \bar{U}'^2)^{\frac{1}{3}}. \quad (82)$$

For the linearly growing portion of the streak, in which u eventually becomes independent of x , this analysis will not hold and the variation of y with time will have to be determined from the full diffusion equation (74) with the term u_{yy} included.

9. Modelling of the nonlinear driving terms

It follows from the above analysis of a convected eddy that, because of the spanwise stretching of the mean shear, local regions of high shear will always arise in a disturbed three-dimensional flow of low viscosity. Such regions can be expected to suffer from local instability of the inflectional type. Because the timescale of such an instability is inversely proportional to the shear, the instability will develop very quickly and thereby provide a local strong mixing that could serve as the intermittent driving term in the model. Although there could also be other mechanisms giving rise to locally strong nonlinear activity, we will assume the dominating one to be local inflectional instability.

Provided the scale of the unstable motion is much smaller than the background large-scale motion which is causing it, one can use the classical hydrodynamic instability theory in conjunction with kinematic wave theory to study the exponential growth of a wave train, or wave group. One thus analyses an instability of the form

$$u = \hat{u}(y) E, \quad v = \hat{v}(y) E, \quad w = \hat{w}(y) E, \quad (83)$$

where

$$E = \exp[i\alpha(x-ct) + i\beta z], \quad c = c_r + ic_i \quad (84)$$

(real part is implied). Slow variations in (x, y) -space and time of the complex amplitudes $\hat{u}, \hat{v}, \hat{w}$ could be incorporated with the aid of kinematic wave theory. The disturbances develop on a parallel flow field of the form

$$U(y) = (U(y), W(y)), \quad U = U + \tilde{u}, \quad W(y) = \tilde{w}, \quad (85)$$

the tilde symbol referring to the large-scale coherent motion which is assumed to vary slowly in (x, z) -space and time. Manipulation of the inviscid linearized disturbance equations in a manner similar to that employed above (57)–(61) in the calculation of the contribution to the Reynolds stress from a local disturbance structure gives

$$-\frac{d}{dy}(\hat{u}\hat{v}^*) = A \sin \Theta_w + B \cos \Theta_w, \quad (86)$$

$$-\frac{d}{dy}(\hat{w}\hat{v}^*) = -A \cos \Theta_w + B \sin \Theta_w, \quad (87)$$

where

$$A = \frac{1}{2} \tan(\Theta_w - \Theta_u) \frac{d}{dy} \left[\tilde{U}''(y) \frac{d}{dt} |\hat{l}|^2 \right], \quad (88)$$

$$B = \frac{1}{2} \tilde{U}'' \frac{d}{dt} |\hat{l}|^2, \quad \frac{d}{dt} |\hat{l}|^2 = \frac{|\hat{v}|^2 c_i}{(\tilde{U} - c_r)^2 + c_i^2}, \quad \alpha \tilde{U} = \alpha U + \beta W. \quad (89)$$

Here $\hat{l}(y)$ is the complex amplitude of the fluid-element liftup and \tilde{U} represents the mean velocity in the direction of the wave. Cross-flow instability may arise when \tilde{U} has an inflection point. The highest growth rate may be expected for waves with wave fronts normal to the local flow direction. Hence, for the most unstable waves

$$\Theta_w \approx \Theta_u, \quad A \approx 0 \quad (90)$$

or, for the total momentum transfer due to the instability,

$$- \int_{t_0}^{t_n} \frac{d}{dy} (u, v^*) Dt \approx \hat{B} \cos \Theta_w, \quad (91)$$

$$- \int_{t_0}^{t_n} \frac{d}{dy} (w, v^*) Dt \approx \hat{B} \sin \Theta_w, \quad (92)$$

where

$$\hat{B} = U'' \frac{1}{2} |\hat{l}|^2. \quad (93)$$

Accordingly, we choose for the conditionally sampled driving term $\langle Q \rangle$:

$$\langle Q \rangle \equiv \frac{\partial^2}{\partial y^2} \left(\frac{\partial}{\partial x} \langle uw \rangle + \frac{\partial}{\partial z} \langle vw \rangle \right) = \frac{\partial^2}{\partial y^2} \left(\frac{\partial \hat{B}}{\partial x} \cos \Theta_w + \frac{\partial \hat{B}}{\partial z} \sin \Theta_w \right), \quad (94)$$

and for \hat{B} a modified Gaussian 'hat',

$$\hat{B} = \hat{C} y^3 \left[1 - 2 \left(\frac{z}{l_3} \right)^2 \right] \exp \left[- \left(\frac{x}{l_1} \right)^2 - \left(\frac{y}{l_2} \right)^2 - \left(\frac{z}{l_3} \right)^2 \right], \quad (95)$$

\hat{C} being an arbitrary constant. The variation with y is the same as that used by Bark (1975). The factor $1 - 2(z/l_3)^2$ is included to make

$$\int_{-\infty}^{\infty} \hat{B} dz = 0,$$

which is necessary in order for the spanwise velocity perturbation to vanish at $z = \pm \infty$. The resulting structure may be subdivided into a symmetrical one, denoted by subscript s, multiplying $\cos \Theta_w$ in (94), and an antisymmetrical one, denoted by subscript a, which multiplies $\sin \Theta_w$. Both of these may be determined from a single base solution, denoted by subscript b, with initial conditions determined from an initial stream function Ψ_0 for the initial cross-flow velocity field given by

$$\Psi_0 = -\frac{1}{2} \hat{C} l_3^2 y^3 \exp \left[- \left(\frac{x}{l_1} \right)^2 - \left(\frac{y}{l_2} \right)^2 - \left(\frac{z}{l_3} \right)^2 \right] \quad (96)$$

such that $(v_b)_{t=0} = -\frac{\partial \Psi_0}{\partial z}, \quad (w_b)_{t=0} = \frac{\partial \Psi_0}{\partial y}.$ (97)

The symmetrical and antisymmetrical portions are then found from

$$v_s = \frac{\partial v_b}{\partial x} \cos \Theta_w, \quad v_a = \frac{\partial v_b}{\partial z} \sin \Theta_w, \quad (98)$$

and similarly for the other components. Since, following (98),

$$\int_{-\infty}^{\infty} v_s(x_1, y, z, 0) dx_1 = 0,$$

only the antisymmetrical portion will be responsible for the streamwise growth of the streaks for large times.

10. Results for the model structures and comparisons with numerical simulations

For the calculation of the evolution of the model streaky structures, the mean velocity and its first and second derivatives are needed. For this the expression proposed by Reichardt (1951) was employed. The initial streamwise velocity component for the disturbance was taken as zero on the assumption that the local instability on the average creates just enough Reynolds stress to remove the streamwise disturbance producing the instability (Landahl 1975). The scale factors l_1 , l_2 , and l_3 were chosen such as to correspond approximately to the conditions in the investigation of Alfredsson *et al.* (1988). In their conditional sampling of the numerically generated data for the streamwise fluctuation component they used the VISA ('variable interval space averaging', the spatial counterpart of VITA) with an integration length of $L^+ = 200$, which they found corresponds approximately to $T^+ = 10$ in the VITA studies of Johansson & Alfredsson (1982). Accordingly, in the present theoretical model, the streamwise scale l_1 was selected such as to make the variance maximum, for a given value of the mean square of the streamwise disturbance velocity component, for that value of the integration time (see Landahl 1984). This gave a value for l_1 of approximately 100 in viscous wall units, which was hence adopted. The vertical scale l_2^+ in the model (98) was chosen as 15, which was found to give a y -distribution of the Reynolds stress in reasonable agreement with the measured Reynolds stresses during bursting found by Kim, Kline & Reynolds (1971). Finally, $l_3^+ = 30$ was selected so as to give a spanwise scale of the u -signature close to what was obtained in the conditional sampling results of Alfredsson *et al.* (1988).

The numerical quadrature of the appearing integrals was carried out with the aid of a cubic-spline-fit routine. Through numerical experimentation it was found that satisfactory accuracy was achieved by representing the integrands in 21 equidistant points between $x^+ = -200$ and $x^+ = 200$ and 21 points between $y^+ = 0$ and $y^+ = 50$. All the results presented were obtained from the near-wall approximation (56). In that, z appears solely as a parameter, so that only one (x, y) -plane for each of the symmetric and antisymmetrical distributions needs to be evaluated, the variation with z determined simply through multiplication with the appropriate functions of z . The step-by-step integration in time was carried out with a step size of $\Delta t^+ = 0.5$. Some test calculations with half this step size produced insignificant differences, showing that the second-order explicit method developed for the time integration gave satisfactory convergence for this step size.

In figures 2-5 are presented results for the evolution of both symmetrical structures, with $\theta = 0^\circ$, and structures having a small amount of asymmetry, $\theta = 5^\circ$. Figure 2 illustrates their early development, at $t^+ = 5$. The u -contour plots for the plane $z = 0$ (figure 2a) shows a region of low speed situated downstream of one of high speed. (Note that for this plane the contours are independent of the obliquity of the initial disturbance since the antisymmetric part of the disturbance is zero in

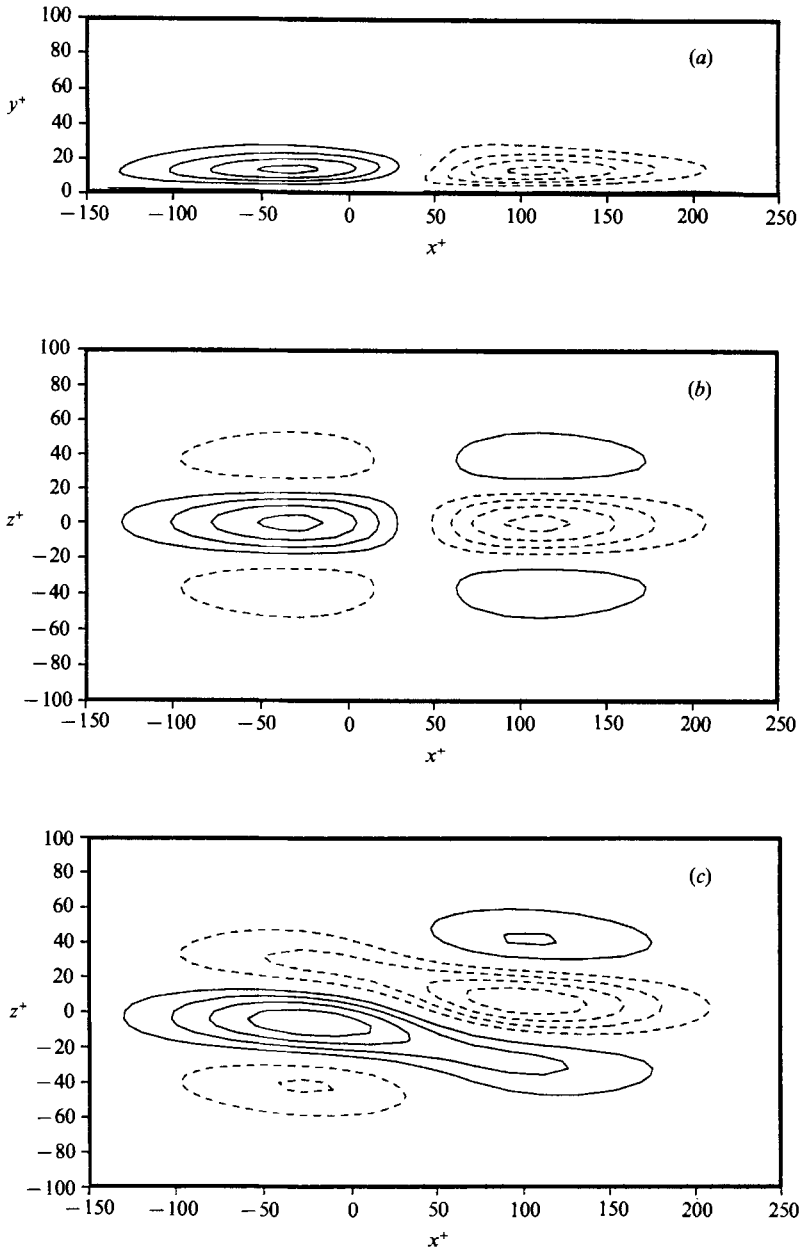


FIGURE 2. Contours of constant u for model structure at $t^+ = 5$: (a) plane $z^+ = 0$, symmetrical and asymmetrical model structure; (b) plane $y^+ = 15$, symmetrical structure ($\theta = 0^\circ$); (c) as (b) but for asymmetrical structure, $\theta = 5^\circ$. Contours start at -0.2 with spacing of 0.05 .

this plane.) The low-speed region results from the liftup of fluid elements ('ejection') and the high-speed region from inflow ('sweep') towards the wall caused by the slowly decaying symmetrical part of the initial v -distribution, see (94). This is also seen in the contour plot of the symmetrical disturbance ($\theta = 0^\circ$) for the plane $y^+ = 15$ (figure 2b). In the corresponding contour plot for the asymmetrical structure, with $\theta = 5^\circ$ (figure 2c), this upstream-sweep downstream-ejection feature is not so clearly marked because it is masked by the strong effect of the antisymmetrical

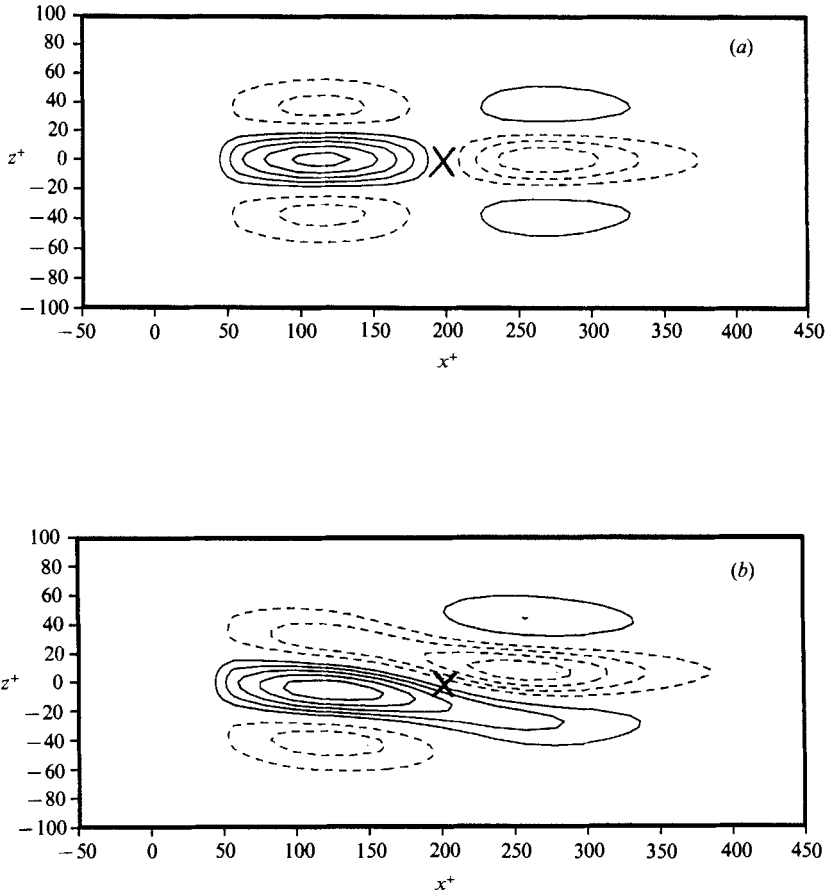


FIGURE 3. Contours of constant u in the plane $y^+ = 15$, $t^+ = 25$: (a) symmetrical structure; (b) asymmetrical structure, $\theta = 5^\circ$. Contours start at -0.8 with spacing of 0.2 .

portion, which makes the pattern dominated by a high-speed region side-by-side in the spanwise direction with a low-speed one, both somewhat tilted in the streamwise direction.

The long-time evolution for $t^+ = 25$ – 60 is illustrated in figures 3–5 which give the u -contours at the plane $y^+ = 15$ for the two kinds of disturbances. The elongation of the asymmetrical structure for $t^+ > 25$ is clearly evident. Also, for large times (figures 4 and 5) the asymmetrical structures have developed an irregular wavy appearance very reminiscent of the long structures found near the wall in the numerical simulations of Moin & Kim (1982). Since these structures are advected downstream with the mean velocity, in a laboratory frame of reference they will appear as oscillations. This result is also in accordance with the experiments of Kline *et al.* (1967) which showed that the streaks began to oscillate before they broke up.

The symmetrical structures, on the other hand, show little, if any, streamwise growth; in contrast, for large times they appear to break up into smaller cells. This behaviour is most evident for the longest time considered, $t^+ = 60$, (see figure 5a) and has the character of a splitting of the structure into cells of about half the original streamwise scale with the cells weakening with increasing distance downstream. This behaviour may be explained by the excitation of damped waves,

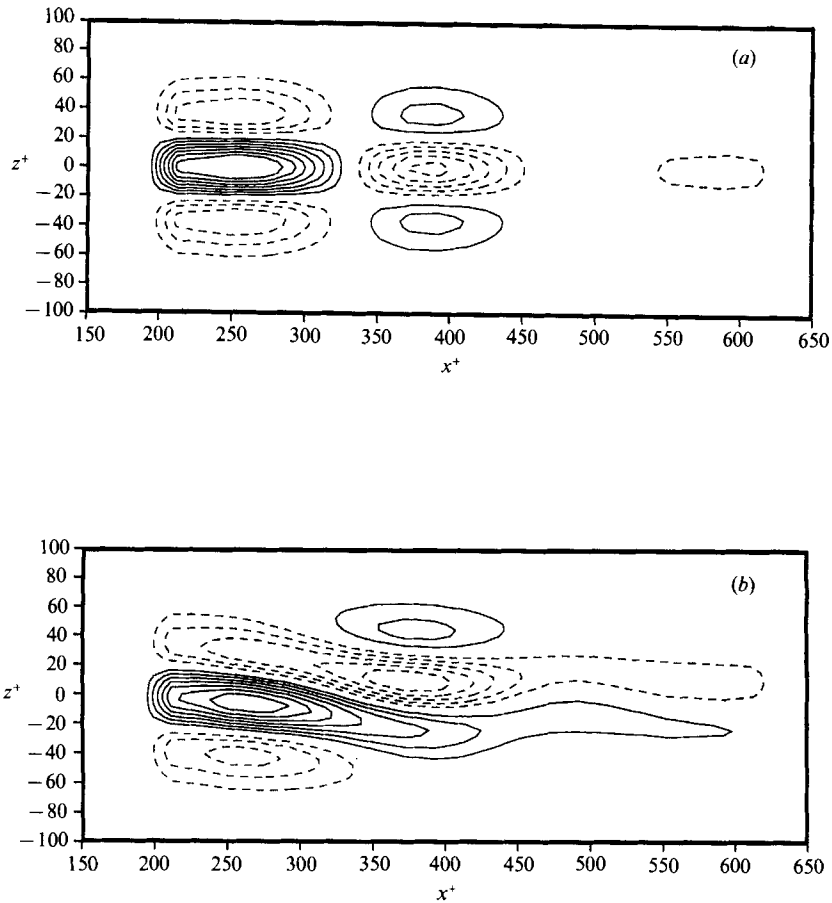


FIGURE 4. Contours of constant u in the plane $y^+ = 15$, $t^+ = 40$: (a) symmetrical structure; (b) asymmetrical structure, $\theta = 5^\circ$. Contours start at -1.0 with spacing of 0.25 .

which is also strongly suggested by the results shown in figure 5c), in which only the transient part of the solution is included, and which do not show this behaviour. Since the transient part of the solution omits the interactive portion taking account of the effect of the curvature of the mean velocity distribution, it cannot incorporate any wave motion.

The results obtained may be compared with those found from numerical simulation of turbulent wall-bounded flows. In figure 6 is reproduced the instantaneous streamwise fluctuation velocity contours for the plane $y^+ = 6.14$ obtained by Moin & Kim (1982) in their Navier-Stokes simulation of turbulent channel flow. The width of the spanwise section shown is approximately 600 in viscous wall units. The spanwise alternation of high- and low-speed elongated regions is clearly evident. Particularly interesting is the wiggly appearance of the longer streaks, also exhibited by the theory for the older structures. This behaviour may be a consequence of the excitation of the damped waves and points to a possible explanation for the streak oscillations seen in the visualization experiments discussed above.

The NASA Ames numerical data bases were also used in the recent investigations by Johansson, Alfredsson & Kim (1988) and Alfredsson *et al.* (1988) to study the near-wall turbulence structure with the use of the VISA conditional sampling

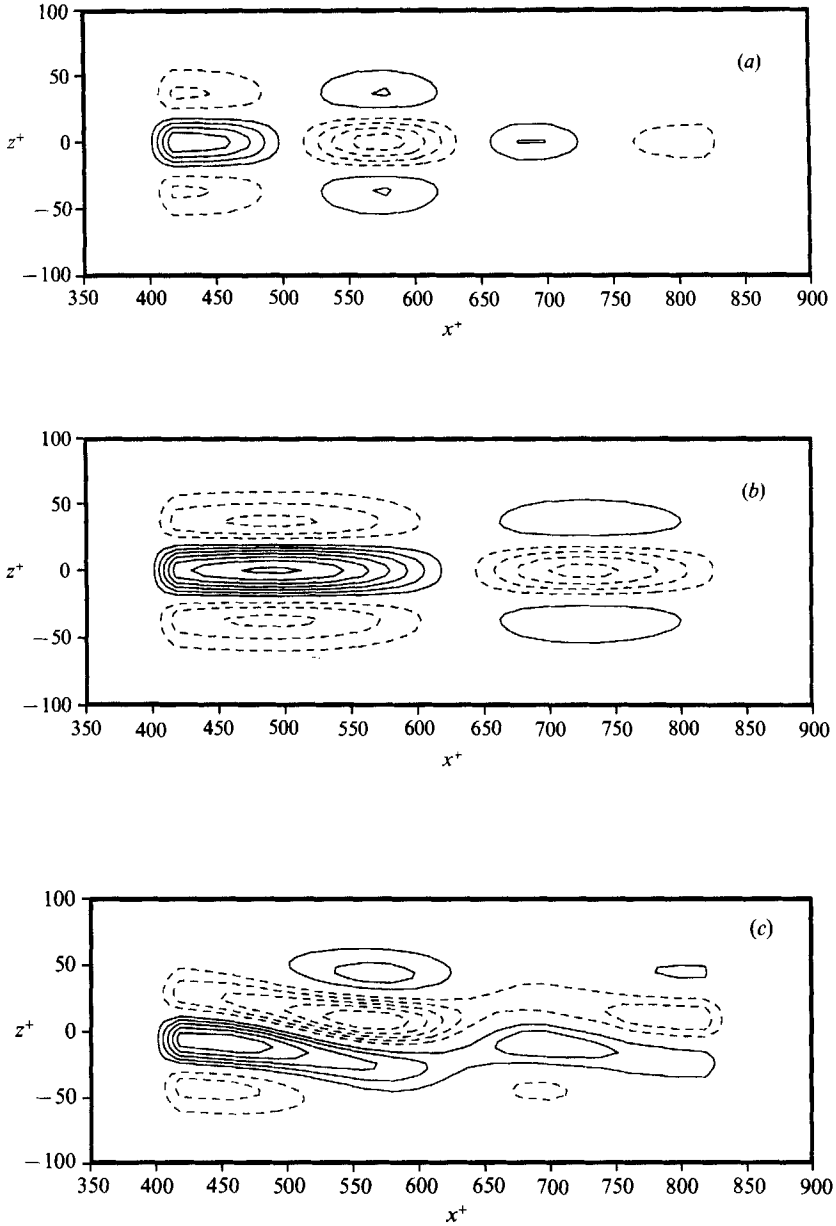


FIGURE 5. Contours of constant u in the plane $y^+ = 15$, $t^+ = 60$: (a) symmetrical structure; (b) symmetrical structure, transient part of the solution; (c) asymmetrical structure, $\theta = 5^\circ$. Contours start at (a) -2.5 , (b) -2.0 , (c) -2.5 with spacing of 0.5 .

technique. The straightforward application of any one-point detection scheme, such as the VITA or VISA, will sort out only structures with spanwise symmetry because of the statistical homogeneity in z of the fluctuating field. However, simple theoretical arguments (Landahl 1975) indicate that asymmetrical structures may be important. In order to study asymmetrical structures, Alfredsson *et al.* (1988) devised a special scheme, in which the individual structures were switched with respect to the (x, y) -midplane according to the sign of the spanwise derivative of u at

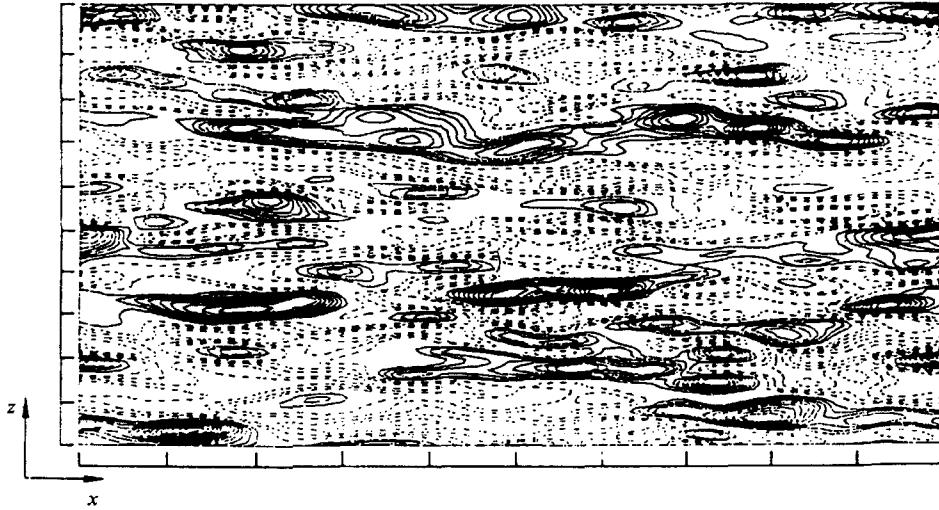


FIGURE 6. Contours of fluctuating streamwise velocities in the plane $y^+ = 6.14$ obtained by numerical simulation for a channel flow. From Moin & Kim (1982).

the detection point. The resulting u -pattern in the $y^+ = 15$ plane (taken from Alfredsson & Johansson 1988) is shown in figure 7(c) at the time of detection of the structure. The corresponding symmetrical structure is illustrated in figure 7(a, b). The point $x^+ = 0$ in their diagram is located at the point of detection, which is approximately at the point where $\partial u / \partial x$ is maximum. In the present theoretical model the maximum in $\partial u / \partial x$ occurs approximately, for $t^+ = 25$, at the point marked with an \times in figure 3(a, b); this point thus corresponds to $x = 0$ in the VISA-educed results of Alfredsson *et al.* (1988). The contours of u from the model for an asymmetric structure with $\theta = 5^\circ$ show a remarkable similarity with those obtained from the conditionally sampled numerical data. The model symmetrical structure ($\theta = 0^\circ$) results are also in good qualitative agreement with the sampled numerical data.

The model structures do differ in details from those exhibited by the statistical analysis of numerically generated flows, however. The model results show a much more abrupt onset of the disturbed region than do the numerically generated ones. This may possibly be a consequence of the extreme temporal intermittency for the nonlinear source term assumed in the idealized model, with a Dirac delta function in time. Also, the sample selected for the construction of the average structure includes disturbances of all different obliquities, which would give rise to a smearing effect on the conditionally averaged structure. Such a smearing will not show up in the model structures, which are calculated for one particular oblique angle.

11. Conclusions

In the model considered the fluctuating flow field is assumed to be governed primarily by the linear interaction with the mean shear, the nonlinearity acting only during a vanishingly short time to supply the initial conditions for the subsequent linear evolution. The justification for such a radical idealization is the observed high intermittency of the v -fluctuations, as reflected in the very high values of the flatness found for the distribution function of this component in the near-wall region, and

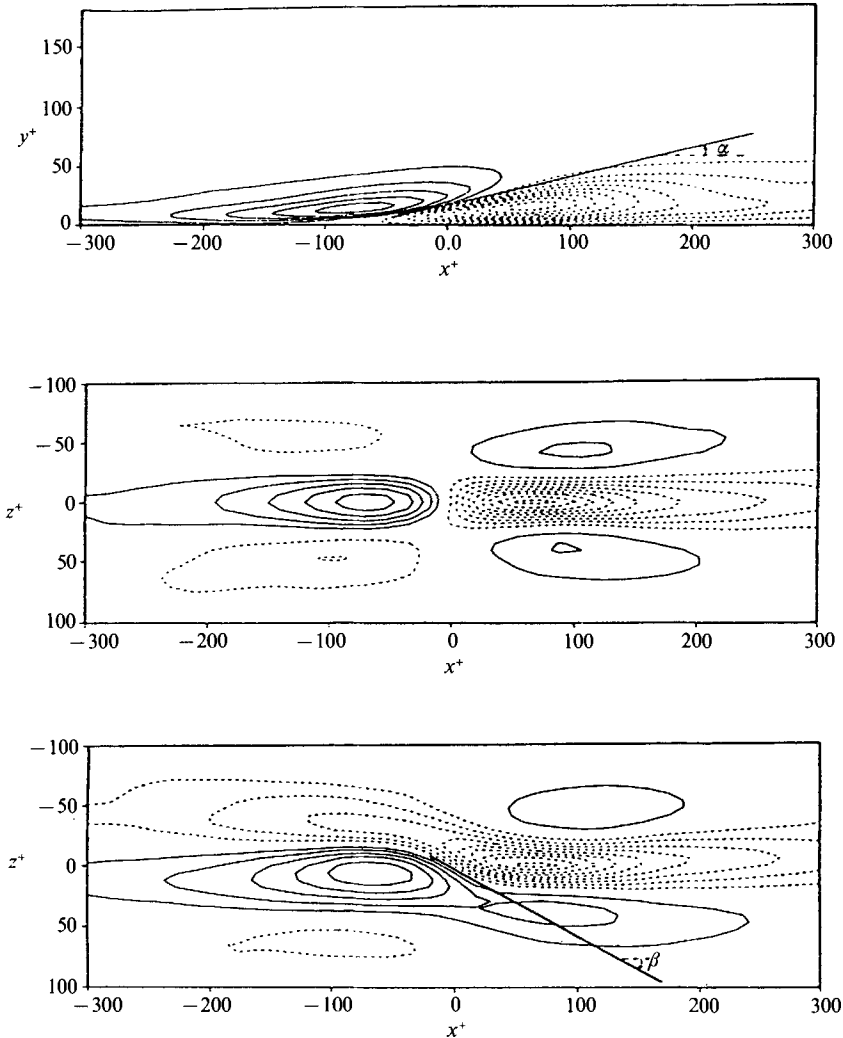


FIGURE 7. Contours of constant u for VISA-educed structures obtained by Alfredsson & Johansson (1988) from numerically simulated turbulent channel flow using the NASA Ames laboratory data bases: (a) detection (x, y)-plane, symmetrical structure; (b) plane $y^+ = 15$, symmetrical structure; (c) $y^+ = 15$, asymmetrical structure.

which is also seen in the bursting phenomenon. It is significant that only the v -component shows this intermittency, the u -component in contrast evolves over a protracted time producing continuously growing streaky regions of low- and high-speed flow.

The formation of the streaky structure was shown to be a direct consequence of algebraic instability (Landahl 1980). Streaks will grow from any initial local and three-dimensional disturbances having a non-zero net vertical momentum along lines of constant y, z . As suggested in an earlier paper (Landahl 1975), such a disturbance could be initiated by a local inflectional instability region with spanwise asymmetry, as would be the case for an oblique wave-like disturbance, perhaps resulting from a cross-flow instability induced by the large-scale spanwise motion.

The Reynolds stress contributed by the streaks may be expressed in a simple

manner in terms of the mean square of the fluid-element liftup, as in Prandtl's mixing-length model. However, the present model gives a different multiplication factor, $(1/2T_b)(\partial U/\partial y)$, T_b being the average time between bursts, to the factor $(\partial U/\partial y)^2$ proposed by Prandtl (1925). The model also suggests that the streaks account for the major part of the Reynolds stresses in the near-wall region, and hence also for the turbulence production.

The structures obtained from the model show a remarkable similarity with those seen in visualization experiments and found from numerical simulations. Thus, the continuous linear growth predicted by the present linear inviscid model is reflected in the longevity, and the large eventual streamwise growth, of the streaks observed both in laboratory and numerical experiments. Also, the irregular wavy appearance of the streaky structures seen in the theoretical model, as well as in the numerical simulations, is strongly suggestive of oscillations that Kline *et al.* (1967) found to occur just before the streak breakup.

The success of a quasi-laminar model like the present one in explaining some of the behaviour of the coherent structures in the turbulent boundary layer suggests the possibility that certain features of turbulent flow may be studied in a laminar environment. This possibility has been explored in the recent Ph.D. dissertation of Breuer (1988) who carried out parallel laboratory, analytical and numerical investigations of a transient three-dimensional localized disturbance in a laminar boundary layer. He found that the downstream evolution of the disturbance was qualitatively similar to the VITA-educed coherent structures in a turbulent boundary layer. He also discovered that the transition to turbulence in such a disturbance, if initially sufficiently strong, follows a different path to that described by the classical one of the growth of a Tollmien-Schlichting wave packet; the stronger disturbance could go through a nonlinear bypass mechanism through the formation of an internal shear layer which would then break down through small-scale inflectional instability.

Support for this research from the Aeronautical Research Institute of Sweden and from NASA Lewis Research Center under Grant No. NCC3-177 is gratefully acknowledged.

This work was completed during the author's sabbatical visits to École Polytechnique Federale in Lausanne, Switzerland, to the NASA Lewis Research Center, to the Aerospace and Mechanical Engineering Department of the University of Arizona, Tucson, and to the Department of Applied Mathematics and Theoretical Physics of the University of Cambridge. The author is most grateful for the warm hospitality he was met by at all these institutions including the use of their computing facilities, and the valuable opportunity to exchange ideas on turbulence and related matters with their researchers.

REFERENCES

- ALFREDSSON, P. H. & JOHANSSON, A. V. 1988 Turbulence experiments – instrumentation and processing of data. In *Proc. 2nd European Turbulence Conference, Berlin, Sept. 1988* (ed. H. Fiedler & H. Fernholz). Springer.
- ALFREDSSON, P. H., JOHANSSON, A. V. & KIM, J. 1988 Turbulence production near walls, the role of flow structures with spanwise asymmetry. In *Proc. 2nd Summer Program of the Center for Turbulence Research*. NASA Ames/Stanford University.
- ASHLEY, H. & LANDAHL, M. T. 1965 *Aerodynamics of Wings and Bodies*. Addison-Wesley.

- BARK, F. H. 1975 On the wave structure of the wall region of a turbulent boundary layer. *J. Fluid Mech.* **70**, 229.
- BLACKWELDER, R. F. & KAPLAN, R. E. 1976 On the wall structure of the turbulent boundary layer. *J. Fluid Mech.* **76**, 89.
- BREUER, K. S. 1988 The development of a localized disturbance in a boundary layer. *MIT FDRL Rep.* 88-1.
- GASTER, M., KIT, E. & WYGNANSKI, I. 1985 Large-scale structures in a forced turbulent mixing layer. *J. Fluid Mech.* **150**, 23.
- GILL, A. E. 1965 A mechanism for instability of plane Couette flow and of Poiseuille flow in a pipe. *J. Fluid Mech.* **21**, 503.
- HARITONIDIS, J. 1989 A model for near-wall turbulence. *Phys. Fluids A* **1**, 302.
- HATZIAVRAMIDIS, D. T. & HANRATTY, T. J. 1979 The representation of the viscous wall region by a regular eddy pattern. *J. Fluid Mech.* **95**, 655.
- JANG, P. S., BENNEY, D. J. & GRAN, R. L. 1986 On the origin of streamwise vortices in a turbulent boundary layer. *J. Fluid Mech.* **169**, 109.
- JOHANSSON, A. J. & ALFREDSSON, P. H. 1982 On the structure of turbulent channel flow. *J. Fluid Mech.* **122**, 295.
- JOHANSSON, A. V., ALFREDSSON, P. H. & KIM, J. 1988 Velocity and pressure fields associated with near-wall turbulence structures. In *Proc. Zoran Zoric Memorial Intl Seminar on Near-Wall Turbulence, May 1988, Dubrovnik*. Springer.
- KIM, H. T., KLINE, S. J. & REYNOLDS, W. C. 1971 The production of turbulence near a smooth wall in a turbulent boundary layer. *J. Fluid Mech.* **50**, 133.
- KLINE, S. J., REYNOLDS, W. C., SCHRAUB, F. A. & RUNSTADLER, P. W. 1967 The structure of turbulent boundary layers. *J. Fluid Mech.* **50**, 133.
- LANDAHL, M. T. 1967 A wave-guide model for turbulent shear flow. *J. Fluid Mech.* **27**, 443.
- LANDAHL, M. T. 1975 Wave breakdown and turbulence. *SIAM J. Appl. Maths* **28**, 775.
- LANDAHL, M. T. 1980 A note on algebraic instability of inviscid parallel shear flows. *J. Fluid Mech.* **98**, 243.
- LANDAHL, M. T. 1984 On the dynamics of large eddies in the wall region of a turbulent boundary layer. In *Turbulence and Chaotic Phenomena in Fluids* (ed. T. Tatsumi), p. 467. Elsevier.
- LANDAHL, M. T. & HENNINGSON, D. S. 1985 The effects of drag reduction measures on boundary layer turbulence structure – implications of an inviscid model. *AIAA-85-0560*.
- LEE, M. J. & HUNT, J. C. R. 1988 The structure of sheared turbulence near a plane boundary. In *Studying Turbulence Using Numerical Simulation Databases – II, Proc. 1988 Summer Program, NASA/Stanford Center for Turbulence Research, Rep.* CTR-S88.
- MOFFATT, H. K. 1965 The interaction of turbulence with strong wind shear. In *Proc. URSI-IUGG Intl Colloquium on Atmospheric Turbulence and Radio Wave Propagation* (ed. A. M. Yaglom & V. I. Tatarsky). Moscow: Nauka.
- MOIN, P. & KIM, J. 1982 Numerical investigation of turbulent channel flow. *J. Fluid Mech.* **118**, 341.
- PRANDTL, L. 1925 Bericht über Untersuchungen zur ausgebildeten Turbulenz. *Z. Angew. Math. Mech.* **5**, 136.
- REICHARDT, H. 1951 Vollständige Darstellung der turbulenten Geschwindigkeitsverteilung in glatten Leitungen. *Z. Angew. Math. Mech.* **31**, 208.
- RUSSELL, J. M. & LANDAHL, M. T. 1984 The evolution of a flat eddy near a wall in an inviscid shear flow. *Phys. Fluids* **27**, 557.
- TAYLOR, G. I. 1915 Eddy motion in the atmosphere. *Phil. Trans. R. Soc. Lond.* **A215**, 1.
- TOWNSEND, A. A. 1976 *The Structure of Turbulent Shear Flow*, 2nd edn. Cambridge University Press.